Deprotection blue in extreme ultraviolet photoresists: Influence of base loading and post-exposure bake temperature

Christopher N. Anderson

Applied Science & Technology Graduate Group,
University of California, Berkeley, Berkeley, CA 94720, USA

Patrick P. Naulleau
Center for X-Ray Optics, Lawrence Berkeley National Laboratory, Berkeley, California 94720, USA

This work was supported by the Director, Office of Science, Office of Basic Energy Sciences, of the U.S. Department of Energy under Contract No. DE-AC02-05CH11231.

Deprotection blur in extreme ultraviolet photoresists: influence of base loading and post-exposure bake temperature

Christopher N. Anderson*

Applied Science & Technology Graduate Group,

University of California, Berkeley, Berkeley, CA 94720, USA

Patrick P. Naulleau

Center for X-ray Optics, Lawrence Berkeley National Laboratory,

1 Cyclotron Road, Berkeley, CA 94720, USA

Abstract

The deprotection blur of Rohm and Haas XP 5435, XP 5271, and XP 5496 extreme ultraviolet photoresists has been determined as their base weight percent is varied. We have also determined the deprotection blur of TOK EUVR P1123 photoresist as the post-exposure bake temperature is varied from 80 °C to 120 °C. In Rohm and Haas XP 5435 and XP 5271 resists 7x and 3x (respective) increases in base weight percent reduce the size of successfully patterned 1:1 line-space features by 16 nm and 8 nm with corresponding reductions in deprotection blur of 7 nm and 4 nm. In XP 5496 a 7x increase in base weight percent reduces the size of successfully patterned 1:1 line-space features from 48 nm to 38 nm without changing deprotection blur. In TOK EUVR P1123 resist, a reduction in post-exposure bake temperature from 100 °C to 80 °C reduces deprotection blur from 21 nm to 10 nm and reduces patterned LER from 4.8 nm to 4.1 nm.

PACS numbers:

*Electronic address: cnanderson@berkeley.edu

I. INTRODUCTION

Resists and processing procedures for extreme ultraviolet (EUV) lithography ($\lambda = 13.5$ nm) are continuously being optimized for the 22 nm manufacturing node. In many ways, however, we still do not have a good understanding of EUV photoresists. Much of the difficulty is that we typically judge resist performance based on the final printed wafer, which of course is a product of the entire coating, exposure, and development process. Deconvolving the effects of the resist, moreover the effects from different constituents within the resist, is often a difficult task.

Over the past four years many metrics have been developed to benchmark resist performance in a variety of areas. One parameter that has received a lot of recent attention is intrinsic resolution (or deprotection blur) as it represents a fundamental limitation in patterning ability. A variety of approaches have been developed to measure deprotection blur in EUV resists: iso-focal bias [1], line-edge roughness (LER) correlation length [2], modulation transfer function (MTF) [3, 4], corner rounding [6, 7], and through-dose contact-hole printing [5–8]. The MTF, corner rounding, and contact-hole metrics have all repeatedly shown consistency with direct observation [6, 9], however the contact-hole metric has several properties that currently make it attractive for large-scale resist comparisons [8].

At the present time it is still unclear how resist deprotection blur influences patterning ability and other observable printing characteristics. Several authors have reported that increased levels of base and photo acid generator (PAG) in EUV resists lead to improved LER and patterning ability [10–12]. In recent work [12], the contact-hole metric was used to monitor the deprotection blur in an experimental open platform resist (EH27 [13]) as the weight percent of base and PAG were varied. No significant change in deprotection blur was observed despite observing performance improvements with increased base/PAG. It is well known, however, that increasing base in EUV photoresist requires higher doses to print the same size features. Consequently, performance improvements with increased base are often attributed to improved photon statistics [10, 11]. Here we will examine three Rohm and Haas resists, monitoring printing fidelity and deprotection blur as base is varied to provide additional data on this unsolved issue.

Another process parameter that has been discussed in the literature, in relation to printing performance and deprotection blur, is the post-exposure bake (PEB) temperature [9].

Previous work has shown at EUV wavelengths that the critical dimension (CD) of resist patterns remaining after development can be sensitive to small changes in PEB temperature [14]. More recent work has shown that several performance metrics, including exposure latitude, resist contrast, RELS [15] and intrinsic blur (measured with the MTF metric) are sensitive to PEB temperature in Rohm and Haas XP 6305A resist [9] . In this report we will monitor the printing fidelity and deprotection blur of TOK EUVR P1123 photoresist as the PEB temperature is varied while keeping track of LER, patterning ability, and dose-to-size.

II. THE CONTACT-HOLE BLUR METRIC

The contact-hole metric has been described in detail in the literature [7, 8] and is only summarized here. The metric involves capturing scanning electron microscope (SEM) images of contact-holes through dose at best focus in the focus-exposure-matrix (FEM) and measuring their average printed diameter (PD) at each dose. Experimental PD vs. dose data is then compared to modeled PD vs. dose data generated using the HOST point-spread function resist blur model [16]. Deprotection blur is determined by finding the programmed blur that minimizes the mean-squared-error between the modeled and experimental PD vs. dose data.

As with most PSF-based resolution metrics, the contact-hole metric requires the ability to accurately model the aerial images that create the experimental printing data. In practice, uncertainties in exposure tool aberrations and focus place constraints on the accuracy to which this can be done. The sensitivity of the contact-hole metric to limitations in aerial image modeling has been previously characterized at the SEMATECH Berkeley MET printing facility [17] assuming 0.15 nm RMS errors in interferometrically measured aberrations [18] and assuming 50 nm focus steps in the FEM [7]. The aerial-image-limited error bars in extracted deprotection blur for the contact-hole metric were reported at 1.25 nm RMS.

Several other error sources associated with the contact metric have been identified and analyzed in previous work [8]. The error bars from these sources have been shown to be the same order as the error-bars due to limitations in aerial image modeling. In addition, a reproducibility experiment has shown that the full-proces error bars for the contact-hole metric are within the 1.75 nm quadrature addition of the reported experimental and modeling error-bars [8].

III. EXPERIMENT AND RESULTS

A. Resists

Through-base resist series' were provided Rohm and Haas and are based on the XP 5435, XP 5271, and XP 5496 resist platforms. Table I summarizes the resist thickness, post-application bake (PAB), post-exposure bake (PEB), and development parameters for each resist platform; these remain fixed for all base weight percents within a particular platform; all process parameters were recommended by the resist supplier. The capital letters next to the Rohm and Haas resists are used to label the relative base weight percents of 0.3, 0.5, 1.0, and 2.0 in each platform; XP 5435 has an additional base level of 4.0 (XP 5435H) [?]. Table I also shows the process parameters for the TOK EUVR P1123 resist used in the PEB temperature study. It is understood that the PEB temperature is varied from the supplier-recommended 90 °C temperature while all other parameters were fixed. Four inch HMDS-primed wafers were used for all experiments and all wafers were developed using a single puddle of Rohm and Haas MF26A developer.

B. Exposures

Exposures were performed at the 0.3 numerical aperture SEMATECH Berkeley microfield exposure tool printing facility at the Advanced Light Source at Lawrence Berkeley National Laboratory using conventional $\sigma = 0.35 - 0.55$ annular illumination [17]. Line-space and contact-hole data were printed using the LBNL 5,2 dark field and LBNL 7,2 dark field masks, respectively. Contact features for the resolution metric were coded to print with a 50 nm diameter and 125 nm pitch (1:1.5 duty cycle). For the determination of patterned LER and intrinsic LER and we use dark-field 1:1 line space patterns with 50 nm half-pitch and 100 nm half-pitch, respectively.

C. Metrology

SEM analysis was performed at LBNL on a Hitachi S-4800 with a working distance of 2 mm and an acceleration voltage of 2.0 kV. All line-space and contact-hole data were characterized using offline analysis software [19]. LER data for line-space patterning is

obtained using a 3x3 dose-focus process window around the center-dose center-focus site in the FEM. In this report we measure two different size line-space patterns: 50 nm half-pitch and 100 nm half-pitch. For 100 nm 1:1 features the SEM magnification is set to 100k providing 6 patterned lines in each SEM image. The reported LER magnitude is the average of the 54 single-line LER values in the process window and the reported LER uncertainty is the 3σ standard deviation of the 54 single-line LER values divided by the square root of the number of lines in the process window. For 50 nm features the SEM magnification is set to 150k providing 8 patterned lines per SEM image and 72 lines in the process window. The spatial frequency spectrum of a single-line LER measurement is confined to a passband with a minimum period of 10 nm (just above the noise floor) and a maximum period of 834 nm (the height of the SEM image).

PD values used for the extraction of deprotection blur with the contact metric are the average PD of 25 central contacts printed in an 8x8 array. All contact metric error sources identified in previous work have been minimized by adhering to suggested process guidelines [8]: all SEM images are well focused, with emission current fixed throughout each through-dose set; SEM electron beam dosing is avoided by focusing in on a local contact site and shifting the field by 1 μm just before image capture; SEM images are gathered by the same person; all PD measurements are made at the same threshold level (0.5) in the image analysis software.

D. Base loading results

Figure 1 shows SEM images of bright field 1:1 lines at best focus printed in Rohm and Haas XP 5435 resist with different base weight percents shown at the left of each row. Figure 2 shows the corresponding data for the XP 5496 platform; line-space printing data for XP 5271 is not shown however it follows similar patterning behavior through base as the presented data. The measured deprotection blurs of the XP 5435, XP 5496, and XP 5271 platforms, through base, as well as other performance metrics, are summarized in Table II. We also include previously reported base loading data for EH27 resist for completeness [12]. Through base, the XP 5435 and XP 5271 platforms experience marginal reductions in deprotection blur while the XP 5496 and EH27 platforms see no statistically significant change in blur. The deprotection blur of XP 5435F is missing because we never exposed

contacts for this resist.

E. PEB results

Figure 3 shows SEM images of bright field 1:1 lines printed through pitch in TOK EUVR P1123 resist for PEB temperatures of 80, 90, 100, and 120 °C. Upon direct inspection of the SEM images, there are some subtle changes in printing performance between the 80 and 100 °C PEB temperatures. Most noticeable by eye is that the semi-isolated (outer) lines start to merge at smaller pitches and eventually fuse as the PEB temperature is increased; LER improvements with decreasing PEB are marginal (see inset in Figure 3). At the 120 °C PEB temperature the semi-isolated lines completely clear at the largest feature size (45 nm) and there is a significant LER increase over the 100 °C LER in the smaller features. Figure 4 shows SEM images of the contact wafer that we printed for blur extraction at the 130 °C PEB temperature. We observed partial lift-off that increased with dose (subfigures a - b) that led to complete lift-off (subfigures c - d). Due to this drastic change in printing behavior we omitted the 130 °C PEB temperature for line-space data.

The deprotection blurs for TOK EUVR P1123 at each PEB temperature, as well as other performance metrics, are summarized near the bottom of Table II. Each PEB experiment was performed at least twice to test reproducibility and the results of each independent blur measurement are summarized in Figure 5. Within the 80-100 °C PEB temperature range, the extracted deprotection blur for repeated trials stays within the reported 1.75 nm RMS error bars of the contact-hole metric [8]. With the exception of the of the 120 °C PEB temperature deprotection blur increases with increased PEB. The blurs at the 120 ° PEB temperature, however, differ by more than the reported error bar [8] so it is likely that at 120 °C were observing the onset of the transition mechanism that shows up at the 130 ° PEB temperature.

IV. DISCUSSION

In Rohm and Haas XP 5435 and XP 5271 resists 7x and 3x (respective) increases in base weight percent reduce the size of successfully patterned 1:1 line-space features by 16 nm and 8 nm with 7 nm and 4 nm reductions in deprotection blur. Given the factor of two difference

between changes in patterning ability and changes in deprotection blur through base, it is unlikely that blur reduction is the underlying mechanism behind improved performance through base in these resists. In support of this conclusion, a 7x increase in base weight percent in Rohm and Haas XP 5496 resist reduces the size of successfully patterned 1:1 line-space features from 48 nm to 38 nm while leaving deprotection blur more-or-less unaffected.

As has been reported in the past [10–12], we observed that increasing the level of base in a given resist increases the dose required for features to print at their coded sizes. It is natural to speculate that improved performance with increased base, correlated to increased doses, is indicative of reduced shot noise. This topic is currently under debate in the literature [10, 12] and we will not discuss it here.

The results of the PEB study agree with the trends presented in previous work [9]. In general, reductions in PEB temperature provide marginal improvements in LER and patterning fidelity at smaller pitches for a tradeoff of reduced sensitivity. When patterning larger (>50 nm) feature sizes, changes in patterning fidelity through PEB temperature are difficult to resolve in top-down SEM images. It is likely that patterning fidelity in larger features also improves with lower PEB temperatures, however we did not obtain the cross sectional data that would be required verify this claim. As the PEB temperatures approach the glass transition, resist performance suffers. At the 120 °C PEB temperature the iso-dense bias increases to the point that the outer lines fuse/clear even though the inner lines can still support the 30 nm 1:1 structure. At the 130 °C PEB temperature liftoff dominates all other failure mechanisms and the majority of the features on the mask cannot print.

V. CONCLUSION

It is unlikely that reduced deprotection blur is the mechanism causing improved patterning and reduced intrinsic LER in EUV resists as base weight percent is increased. Of four resists studied, two showed changes in deprotection blur through base, however, the changes in blur were not large enough to account for observed patterning improvements. None of the resists we have studied perform at the resolution limit as determined by deprotection blur; this suggests that other mechanisms are currently dominating patterning. Reduced PEB temperatures can provide marginal improvements in printing performance for features pushing the limits of the resist at the cost of reduced photospeed.

VI. ACKNOWLEDGMENTS

The authors are greatly indebted to Paul Denham, Ken Goldberg, Brian Hoef, Gideon Jones, and Jerrin Chiu of the Center for X-Ray Optics at Lawrence Berkeley National Laboratory for expert support with the exposure tool as well as the entire CXRO engineering team for building and maintaining the EUV exposure tool. The authors also acknowledge Jim Thackeray and Katherine Spear from Rohm and Haas, and Koki Tamura, Chris Rosenthal, and Dave White at TOK for supplying resist and process support. The authors also acknowledge Robert Brainard and Gregg Gallatin for valuable discussions related to this work. The authors are grateful for support from the NSF EUV Engineering Research Center. This research was performed at Lawrence Berkeley National Laboratory using the SEMATECH-supported MET exposure facility at the Advanced Light Source. Lawrence Berkeley National Laboratory is operated under the auspices of the Director, Office of Science, Office of Basic Energy Science, of the US Department of Energy.

---

[1] G. M. Schmid, M. D. Stewart, C. Wang, B. D. Vogt, M. Vivek, E. K. Lin, C G Willson, "Resolution limitations in chemically amplified photoresist systems," Proc. SPIE 5376, 333-342 (2004).

[2] G. F. Lorusso, P. Leunissen, M. Ercken, C Delvaux, F.V. Roey, N. Vandenbroeck, "Spectral analysis of line width roughness and its applications to immersion lithography," J. Microlith., Microfab., Microsyst., 5(2) (2006).

[3] J. Hoffnagle, W. D. Hinsberg, F. A. Houle, and M. I. Sanchez, "Characterization of photoresist spatial resolution by interferometric lithography", Proc. SPIE 5038, 464-472 (2003).

[4] T. Brunner, C. Fonseca, N. Seong, M. Burkhardt, "Impact of resist blur on MEF, OPC and PD control," Proc. SPIE 5377, (2004).

[5] P. Dirsken, J. Braat, A. J.E.M. Janssen, A. Leeuwestein, H. Kwinten, and D. V. Steenwinckel, "Determination of resist parameters using the extended Nijboer-Zernike theory," Proc. of SPIE 5377 150-159 (2004).

[6] P. Naulleau and C. Anderson "Lithographic metrics for the determination of intrinsic resolution limits in EUV resists," Proc. SPIE 6517, (2007).

[7] C. Anderson and P. Naulleau, "Sensitivity study of two high-throughput resolution metrics for photoresists," Appl. Opt. Vol 47, No. 1 (2008).

[8] C. Anderson and P. Naulleau, "A high-throughput contact-hole resolution metric for photoresists: full-process sensitivity study," Proc. SPIE 6923 (2008).

[9] T. Wallow, R. Kim, B. La Fontaine, P. Naulleau, C. Anderson, R. Sandberg, "Progress in EUV Photoresist Technology," Proc SPIE 6533, 653317 (2007).

[10] R. Brainard, P. Trefonas, J. Lammers, C. Cutler, J. Mackevich, A. Trefonas, and S. Robertson, "Shot noise, LER and quantum efficiency of EUV photoresists," Proc. SPIE 5374 (2004).

[11] D. Steenwinckel, J. Lammers, T. Koehler, R. Brainard, and P. Trefonas, "Resist effects at small pitches," JVST B 24 (1) Jan/Feb (2006).

[12] C. Anderson, P. Naulleau, D. Naikoula, E. Hassanien, R. Brainard, G. Gallatin, K. Dean, "Influence of base and photoacid generator on deprotection blur in EUV photoresists and some thoughts on shot noise" Accepted for publication JVST B 26(6) MS-35934 Nov/Dec (2008)

[13] R. Brainard, E. Hassanein, J. Li, P. Pathak, B. Thiel, F. Cerrina, R. Moore, M. Rodriguez, B. Yakshinskiy, E. Loginova, T. Madey, R. Matyi, M. Malloy, A. Rudack, P. Naulleau, A. Wuest, K. Dean, "Photons, electrons and acid yields in EUV photoresists: a progress report," Proc. SPIE 6923 (2008).

[14] J. Cain, P. Naulleau, C. Spanos, "Critical dimension sensitivity to post-exposure bake temperature variation in EUV photoresists," Proc. SPIE 5751 (2005).

[15] A. R. Pawloski, A. Acheta, I. Lalovic et al., "Characterization of line edge roughness in photoresist using an image fading technique, Proc. SPIE 5376, 414 (2004)

[16] C. Ahn, H. Kim, and K. Baik, "A novel approximate model for resist process," Proc. SPIE 3334, 752763 (1998).

[17] P. Naulleau "Status of EUV micro-exposure capabilities at the ALS using the 0.3-NA MET optic," Proc. SPIE 5374, 881-891 (2004).

[18] K. Goldberg, P. Naulleau, P. Denham, S. Rekawa, K. Jackson, E. Anderson, and J. Alexander Liddle. "At-Wavelength Alignment and Testing of the 0.3 NA MET Optic, J. Vac. Sci. and Technol. B 22, 2956-2961 (2004).

[19] SuMMIT software is distributed by EUV Technology, Martinez, CA 94553, http://www.euvl.com/summit

[20] P. Naulleau, C. Anderson, K. Dean, P. Denham, K. Goldberg, B. Hoef, B. La Fontaine, T. Wallow, "Recent results from the Berkeley 0.3-NA EUV microfield exposure tool," Proc SPIE 6517, (2007).

[21] R. Lawson, C. Lee, W. Yueh, L. Tolbert, C. Henderson, "Mesoscale simulation of molecular glass photoresists: effect of PAG loading and acid diffusion coefficient," Proc. SPIE 6923 (2008)

[] To perhaps clarify the nomenclature, the letter J corresponds to base weight percents of 2.0 and 0.3 in the XP 5496 and XP 5271 platforms, respectively.

List of Figures

List of Tables

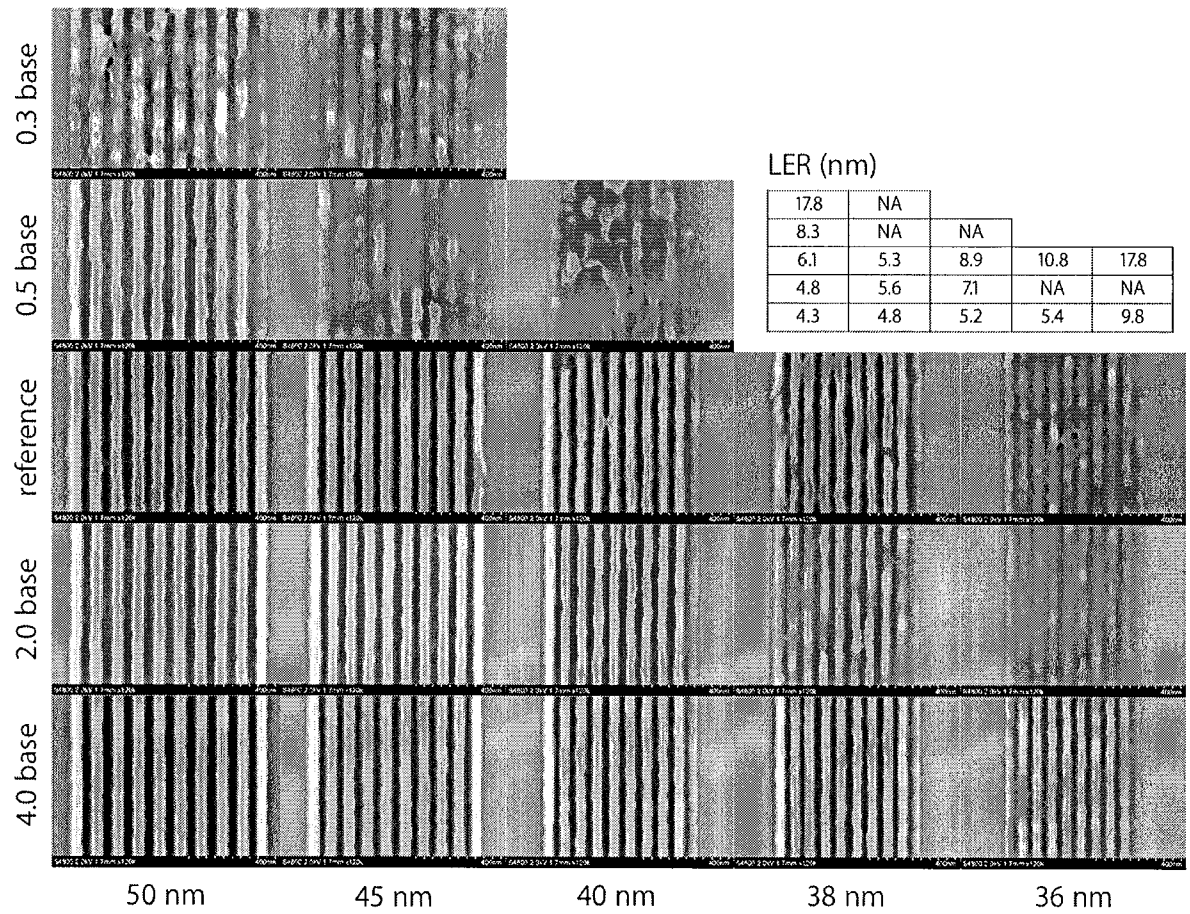

FIG. 1: Base loading study. Through-pitch SEM images of bright field 1:1 lines printed in Rohm and Haas XP 5435 resist. Relative base weight percents are indicated to the left of each row. Half-pitch coded feature sizes are indicated at the bottom of each column. LER information for each SEM image is indicated in the table; note that these LER values are not the same as the process-window-averaged LER values reported in Table II.

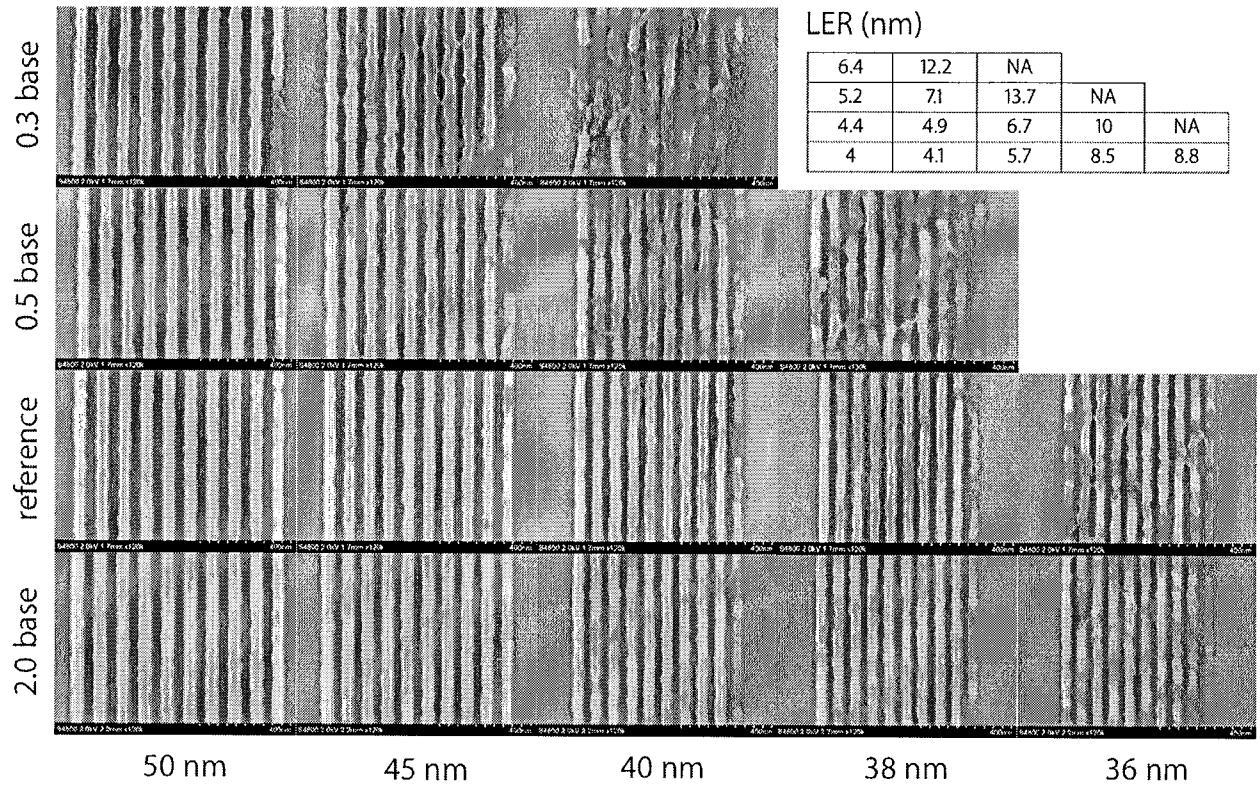

FIG. 2: Base loading study. Through-pitch SEM images of bright field 1:1 lines printed in Rohm and Haas XP 5496 resist. Relative base weight percents are indicated to the left of each row. Half-pitch coded feature sizes are indicated at the bottom of each column. LER information for each SEM image is indicated in the table; note that these LER values are not the same as the process-window-averaged LER values reported in Table II.

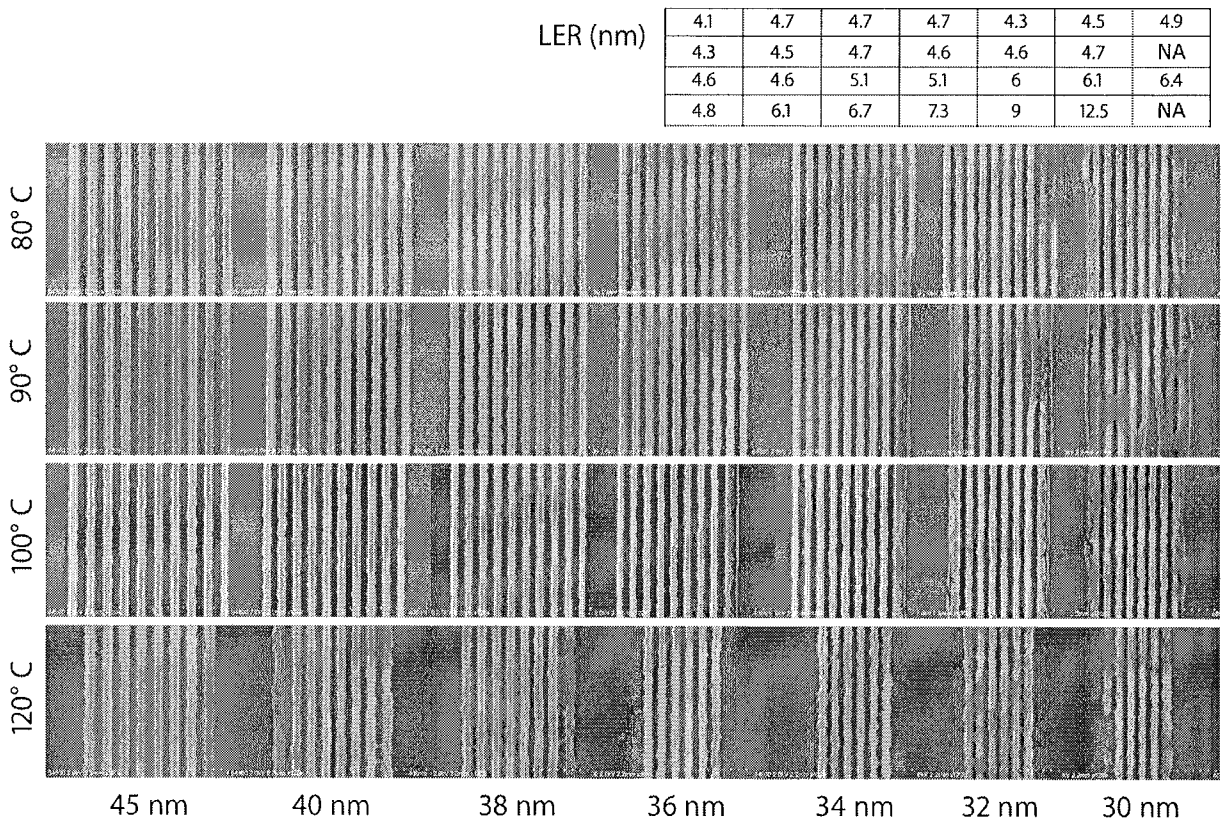

FIG. 3: Post exposure bake (PEB) temperature study. Through-pitch SEM images of bright field 1:1 lines printed in TOK EUVR P1123 resist with PEB temperatures of 80, 90, 100 and 120 °C. The bake time is 90 seconds for all temperatures. Half-pitch coded feature sizes are indicated at the bottom of each column. LER information for each SEM image is indicated in the table; note that these LER values are not the same as the process-window-averaged LER values reported in Table II

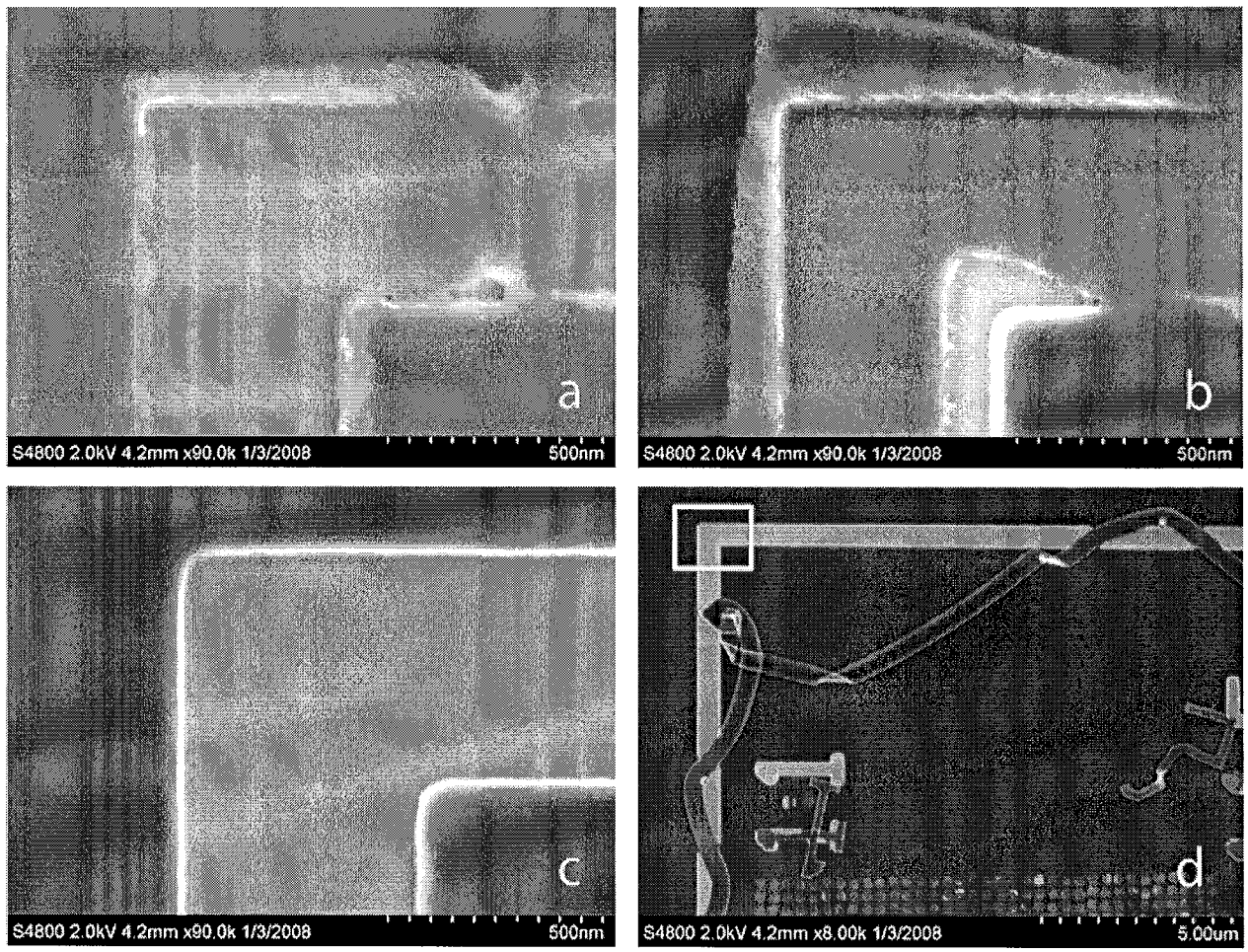

FIG. 4: Post exposure bake (PEB) temperature study. Subfigures a through c are SEM images of a coded 500 nm elbow printed in TOK EUVR P1123 resist with a 130 °C / 90 second PEB with relative dose steps of 1.15 between each image; d is a zoomed out version of c where the field shown in c is outlined in white.

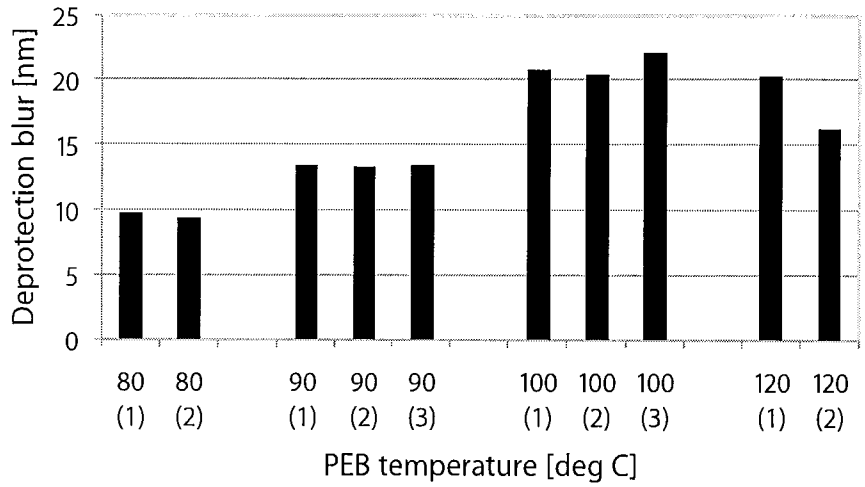

FIG. 5: Post exposure bake (PEB) temperature study. Measured deprotection blur of TOK P1123 resist with PEB temperatures of 80, 90, 100 and 120 °C. Each experiment was performed at least twice to test reproducibility.

TABLE I: Process parameters for reference resist formulations.

Supplier	Resist	Thickness (nm)	PAB (°C)	PEB (°C)	PEB (sec)	Dev. time (sec)
Rohm and Haas	XP 5435 E,F,D,G,H	120	130	130	90	45
Rohm and Haas	XP 5271 J,K,D,L	80	130	120	90	45
Rohm and Haas	XP 5496 H,I,F,J	80	130	90	90	45
TOK	EUVR P1123	60	120	80, 90, 100, 120, 130	90	60

TABLE II: EUV resist performance metrics

Resist	Base % (relative)	Blur (nm)	Pattern limit (nm 1:1)	LER (nm) 50 nm 1:1	LER (nm) 100 nm 1:1	E-size (mJ/cm^2)
XP 5435-E	0.3	32.1	52	10.7 ± 0.6	6.5 ± 0.1	1.6
XP 5435-F	0.5	N/A	50	8.2 ± 0.4	5.8 ± 0.1	2.3
XP 5435-D	1.0	31.3	42	6.1 ± 0.3	5.7 ± 0.2	3.2
XP 5435-G	2.0	26.2	40	5.5 ± 0.3	4.6 ± 0.1	6.4
XP 5435-H	4.0	25.1	36	5.0 ± 0.3	4.0 ± 0.1	14.0
XP 5271-J	0.3	27.9	47	13.4 ± 0.8	8.0 ± 0.2	4.0
XP 5271-K	0.5	25.4	43	6.7 ± 0.3	5.3 ± 0.1	6.5
XP 5271-D	1.0	23.8	39	6.7 ± 0.2	5.2 ± 0.1	12.5
XP 5496-H	0.3	26.5	48	8.1 ± 0.3	7.6 ± 0.1	3.0
XP 5496-I	0.5	26.4	44	7.9 ± 0.3	6.9 ± 0.1	4.7
XP 5496-F	1.0	24.6	38	6.5 ± 0.3	5.8 ± 0.1	7.6
XP 5496-J	2.0	25.0	38	5.3 ± 0.3	5.0 ± 0.1	15.2
EH27-C	0.3	17.0	52	13.4 ± 0.7	6.9 ± 0.1	1.9
EH27-D	0.7	17.3	47	8.8 ± 0.4	5.8 ± 0.1	3.2
EH27-E	1.0	16.7	43	6.8 ± 0.2	4.9 ± 0.1	6.4
EH27-F	1.5	15.0	42	5.3 ± 0.1	4.9 ± 0.1	7.8
EH27-G	2.0	17.1	39	4.5 ± 0.1	4.1 ± 0.1	10.7
P1123 (80° PEB)	1.0	9.7	28	4.3 ± 0.1	4.0 ± 0.1	11.9
P1123 (90° PEB)	1.0	13.5	28	4.5 ± 0.1	4.0 ± 0.1	8.8
P1123 (100° PEB)	1.0	21.1	30	4.8 ± 0.1	4.1 ± 0.1	8.2
P1123 (120° PEB)	1.0	18.3	30	4.8 ± 0.1	N/A	6.8